

Coherent tunnelling conductance in normal-metal/d-wave superconductor/normal-metal double tunnel junctions

This article has been downloaded from IOPscience. Please scroll down to see the full text article.

2004 J. Phys.: Condens. Matter 16 6099

(<http://iopscience.iop.org/0953-8984/16/34/009>)

View [the table of contents for this issue](#), or go to the [journal homepage](#) for more

Download details:

IP Address: 129.252.86.83

The article was downloaded on 27/05/2010 at 17:15

Please note that [terms and conditions apply](#).

Coherent tunnelling conductance in normal-metal/d-wave superconductor/normal-metal double tunnel junctions

Z C Dong^{1,2}, Z M Zheng^{1,3} and D Y Xing^{1,3}

¹ National Laboratory of Solid State Microstructures, Nanjing University, Nanjing 210093, People's Republic of China

² Department of Physics, Huaiyin Teachers College, Huaiyin 223001, People's Republic of China

³ Department of Physics, Nanjing University, Nanjing 210093, People's Republic of China

Received 23 February 2004

Published 13 August 2004

Online at stacks.iop.org/JPhysCM/16/6099

doi:10.1088/0953-8984/16/34/009

Abstract

Taking simultaneously into account the electron-injected current from one normal-metal (N) electrode and the hole-injected current from the other N electrode, we study the coherent tunnelling conductance and quantum interference effects in N/d-wave superconductor (S)/N double tunnel junctions. It is found that oscillations of all quasiparticle transport coefficients and the conductance spectrum with quasiparticle energy and thickness of the d-wave S depend to a great extent on the crystal orientation of the d-wave S. The zero-bias conductance peak is gradually lowered with increasing barrier strength and/or temperature, its magnitude exhibiting damped oscillatory behaviour with thickness of S.

1. Introduction

Quantum interference effects of the quasiparticle transport in double tunnel junctions consisting of superconductor (S) and normal metal (N) have attracted much attention since early experiments by Tomasch [1]. The coherent tunnelling has been studied in S/N/S double tunnel junctions by considering current-carrying Andreev bound states [2, 3] and multiple Andreev reflections (AR) [4–7]. The geometric resonance nature of differential conductance oscillations in the S/N/S [8–10], N/S/N [11], and ferromagnet (F)/F/S [12] double tunnel junctions has been ascribed to the quasiparticle interference in the central film. Recently, the McMillan–Rowell oscillations were observed in S/N/S edge junctions with S having d-wave symmetry, and used for measurements of the superconducting gap and Fermi velocity [13].

Very recently, the study of the coherent quantum transport has been extended to F/s-wave S/F [14–16] double tunnel junctions. It was pointed out [15] that for an F/S/F double tunnel junction, if only the injection of electrons from the left-hand F to S is taken into account, the

current continuous condition cannot be satisfied, which arises from the creation and annihilation of Cooper pairs in S. To solve this difficulty, in the presence of a voltage drop between two F electrodes, not only the electron injection from one F electrode to S, but also hole injection from the other F electrode to S, needs to be taken into account [11, 15]. Several important features have been revealed. The quantum interference effects of quasiparticles in S give rise to oscillations of reflection and transmission probabilities as well as conductances with energy above the superconducting gap, and the AR and corresponding transmission coefficients show periodic vanishing phenomena. In the tunnel limit, all the reflection and transmission coefficients exhibit some sharp peaks, corresponding to a series of bound states of quasiparticles in S. A similar but somewhat different approach [16] was applied to the same F/S/F structure, in which both electron and hole injections from the left-hand F to S were taken into account. If the exchange splitting of F is taken to be zero, both the approaches [15, 16] are equivalent to each other, reducing to the Lambert approach to the N/S/N structures [11]. The theories above dealt with isotropic *s*-wave S, and the quantum coherent effects in the *d*-wave S interlayer have not yet been studied. It is known that the transport properties in the *d*-wave S junctions are quite different from the *s*-wave S junctions. In *a*-*b* plane junctions of the *d*-wave S, not only the magnitude of the pair potential but also the orientation of the S crystal with respect to the interface normal influence significantly the quasiparticle interference in the junction. Owing to the orientation dependence of the pair potential, a most remarkable effect in tunnelling experiments of the high- T_c S is the existence of the zero-bias conductance peak (ZBCP) for $\alpha = \pi/4$ where α is the angle between the *a* axis of the S crystal and the interface normal with the *c* axis fixed within the interface [2, 17, 18]. It was pointed out by a theory of tunnelling conductance [19] that the origin of the ZBCP is the zero-energy state (ZES) formed on the interface of the *d*-wave S where quasiparticles feel the change in sign of the pair potential before and after scattering [20]. It is interesting to clarify how the ZES influences the coherent quantum transport in N/*d*-wave S/N junctions.

In this paper, we will present a theory of the coherent quantum transport in N/*d*-wave S/N double tunnel junctions, and derive a general formula for the differential conductance in terms of reflection and transmission coefficients. We take simultaneously into account the electron-injected current from one N electrode to S and the hole-injected current from the other N electrode to S, as shown in figures 1(a) and (b) (or 1(d) and (c)). In this case, the chemical potential in S is determined by current continuous conditions, i.e., the current from the left-hand N to S via the left-hand N/S interface must be equal to that from S to the right-hand N via the right-hand interface. In the present coherent transport, since the coherent length in the *d*-wave S is much shorter than that in the *s*-wave S, the quasiparticle interference and resonant tunnelling play an important role, exhibiting new quantum effects on the tunnelling conductance in the N/*d*-wave S/N structures.

2. Quasiparticle transport coefficients

Consider an N/*d*-wave S/N double tunnel junction, in which the left- and right-hand electrodes are made of the same N and they are separated from the central S by two thin insulating interfaces, respectively. The N layers are assumed to be the *y*-*z* plane and to be stacked along the *x* direction. The *a*-*b* plane of the *d*-wave S is normal to the *y*-*z* plane. The two very thin insulating layers at $x = 0$ and L can be modelled to be two δ -type barrier potentials: $U(x) = U_0[\delta(x) + \delta(x - L)]$, where L is the thickness of S, and U_0 depends on the product of barrier height and width. As in the previous works [21, 22], we neglect for simplicity the self-consistency of spatial distribution of the pair potential in S and take it as a step function: $\Delta(x, \theta) = \Delta_{\pm}\Theta(x)\Theta(L - x)$ where $\Delta_{\pm} = \Delta \cos(2\theta \mp 2\alpha)$ [19] correspond

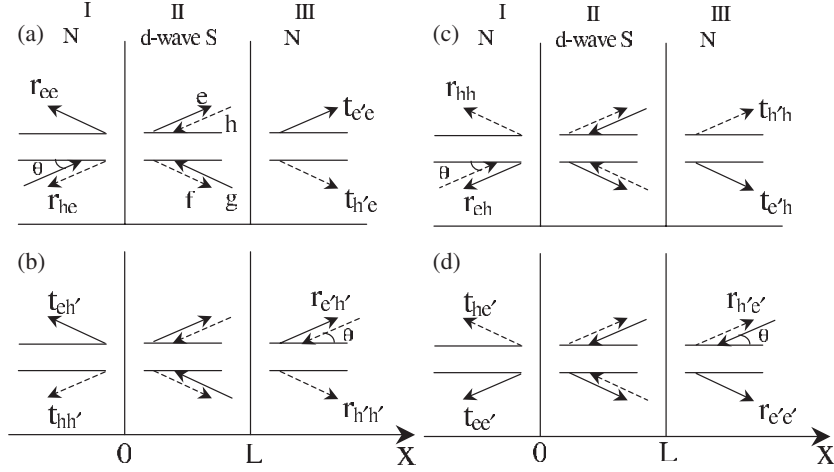


Figure 1. Schematic illustration of reflections and transmissions of quasiparticles in an N/d-wave S/N structure.

to the pair potentials for electron-like and holelike quasiparticles, respectively, with θ the angle between the quasiparticle momentum and the N/S interface normal. We assume that the temperature-dependent gap of S is given by $\Delta = \Delta_0 \tanh(1.74\sqrt{T_c/T - 1})$ [23], where Δ_0 is the superconducting gap at $T = 0$, and T_c is the superconducting critical temperature.

We adopt the Bogoliubov–de Gennes (BdG) approach [24] to study the transport of quasiparticles in the N/d-wave S/N structure. The two-component BdG equation for electron-like and holelike quasiparticle wavefunctions (u, v) is given by

$$\begin{bmatrix} H_0(\mathbf{r}) & \Delta(x, \theta) \\ \Delta^*(x, \theta) & -H_0^*(\mathbf{r}) \end{bmatrix} \begin{bmatrix} u(x, \theta) \\ v(x, \theta) \end{bmatrix} = E \begin{bmatrix} u(x, \theta) \\ v(x, \theta) \end{bmatrix}, \quad (1)$$

where $H_0(\mathbf{r}) = -\hbar^2 \nabla_r^2 / 2m + V(\mathbf{r}) - E_F$ with $V(\mathbf{r})$ the usual static potential, and the excitation energy E is measured relative to the Fermi energy E_F .

Consider an electron incident on the interface at $x = 0$ from the left-hand N at angle θ to the interface normal. As shown in figure 1(a), there are four possible trajectories: the normal reflection (r_{ee}), AR (r_{he}), and transmissions to the right-hand electrode as an electron-like quasiparticle ($t_{e'e}$) and as a holelike quasiparticle ($t_{h'e}$), where subscripts e (h) and e' (h') indicate the electron (hole) in the left- and right-hand N electrodes, respectively. With general solutions of the BdG equation (1), the wavefunctions in the three regions have the following form:

$$\Psi_I = \begin{pmatrix} 1 \\ 0 \end{pmatrix} e^{iq_+ x \cos \theta} + r_{he} \begin{pmatrix} 0 \\ 1 \end{pmatrix} e^{iq_- x \cos \theta} + r_{ee} \begin{pmatrix} 1 \\ 0 \end{pmatrix} e^{-iq_+ x \cos \theta}, \quad (2)$$

for $x < 0$;

$$\begin{aligned} \Psi_{II} = & e \begin{pmatrix} u_+ e^{i\phi_+} \\ v_+ \end{pmatrix} e^{ik_+ x \cos \theta} + f \begin{pmatrix} v_- e^{i\phi_-} \\ u_- \end{pmatrix} e^{-ik_- x \cos \theta} \\ & + g \begin{pmatrix} u_- e^{i\phi_-} \\ v_- \end{pmatrix} e^{-i\bar{k}_+ x \cos \theta} + h \begin{pmatrix} v_+ e^{i\phi_+} \\ u_+ \end{pmatrix} e^{i\bar{k}_- x \cos \theta}, \end{aligned} \quad (3)$$

for $0 < x < L$; and

$$\Psi_{III} = t_{e'e} \begin{pmatrix} 1 \\ 0 \end{pmatrix} e^{iq_+ x \cos \theta} + t_{h'e} \begin{pmatrix} 0 \\ 1 \end{pmatrix} e^{-iq_- x \cos \theta}, \quad (4)$$

for $x > L$. Here $q_{\pm} = \sqrt{2m(E_F \pm E)}/\hbar$ are the wavevectors for the electron and hole in N and $k_{\pm} = \sqrt{2m(E_F \pm \sqrt{E^2 - |\Delta_{\pm}|^2})}/\hbar$ and $\bar{k}_{\pm} = \sqrt{2m(E_F \pm \sqrt{E^2 - |\Delta_{\mp}|^2})}/\hbar$ are the wavevectors for the electron-like and holelike quasiparticles in S. $(u_{\pm})^2 = 1 - (v_{\pm})^2 = (1 + \sqrt{1 - |\Delta_{\pm}/E|^2})/2$ and $\phi_{\pm} = \cos^{-1}[\cos 2(\theta \mp \alpha)/|\cos 2(\theta \mp \alpha)|]$.

All the coefficients in equations (2)–(4) can be determined by boundary conditions at $x = 0$ and L . The matching conditions for the wavefunctions are given by $\Psi_{\text{II}}(0) = \Psi_{\text{I}}(0)$, $(d\Psi_{\text{II}}/dx)_{x=0} - (d\Psi_{\text{I}}/dx)_{x=0} = 2mU_0\Psi_{\text{I}}(0)/\hbar^2$, $\Psi_{\text{III}}(L) = \Psi_{\text{II}}(L)$, and $(d\Psi_{\text{III}}/dx)_{x=L} - (d\Psi_{\text{II}}/dx)_{x=L} = 2mU_0\Psi_{\text{III}}(L)/\hbar^2$. The probabilities of the AR, normal reflection, and transmission from the left-hand N to the right-hand N as an electron and a hole are given by $R_{\text{he}} = (q_-/q_+)|r_{\text{he}}|^2$, $R_{\text{ee}} = |r_{\text{ee}}|^2$, $T_{\text{e'e}} = |t_{\text{e'e}}|^2$, and $T_{\text{h'e}} = (q_-/q_+)|t_{\text{h'e}}|^2$, respectively. Quasiparticle transport coefficients shown in figures 1(b)–(d) can be obtained by similar calculations. Since analytical results for these coefficients are tedious, we only give their numerical results below. From electron–hole scattering symmetries as well as our calculation results, we have $R_{\text{ee}} = R_{\text{e'e'}}$, $R_{\text{hh}} = R_{\text{h'h'}}$, $R_{\text{eh}} = R_{\text{he}} = R_{\text{e'h'}}$, and $T_{\text{e'e}} = T_{\text{e'e'}}$, $T_{\text{h'h}} = T_{\text{h'h'}}$, $T_{\text{h'e}} = T_{\text{eh'}}$, $T_{\text{e'h}} = T_{\text{he'}}$. For either $\alpha = 0$ or $\pi/4$, we have $|\Delta_+| = |\Delta_-|$, so that $k_+ = \bar{k}_+$ and $k_- = \bar{k}_-$. In these cases, it is easily shown analytically that all the coefficients of electron–hole transformation such as R_{he} and $T_{\text{h'e}}$ are proportional to $\sin^2[(k_+ - k_-)L \cos \theta/2]$, which vanish if $(k_+ - k_-)L \cos \theta = 2n\pi$ with n an arbitrary positive integer. From the expressions for k_+ and k_- given above, this condition is equivalent to

$$\left[\frac{E}{\Delta(\theta, \alpha)} \right]^2 = \left[\frac{2\pi n E_F / \Delta(\theta, \alpha)}{k_F L \cos \theta} \right]^2 + 1, \quad (5)$$

under which there is neither an AR nor a hole (electron) transmission so that the quasiparticles pass directly from one N electrode to the other, not converting to the Cooper pair in S. The oscillation period is increased with E , approaching $2\pi E_F / [\Delta(\theta, \alpha) k_F L \cos \theta]$ for $E \gg \Delta(\theta, \alpha)$.

The calculated results for these coefficients as a function of E are plotted in figure 2 (the left-hand column for $\alpha = \theta = 0$ and the right-hand one for $\alpha = \theta = \pi/4$) with different barrier strength $z_0 = mU_0/(\hbar^2 k_F)$. All of them exhibit oscillatory behaviour due to the coherent tunnelling through the N/S/N structure. The other parameters used in the calculation are $E_F/\Delta_0 = 10$ [25] and $k_F L = 100$. It is found that with z_0 increased from zero to unity, each peak in R_{he} splits across, and in the tunnel limit ($z_0 = 2$) each split peak becomes two sharp peaks, corresponding to a series of bound states of quasiparticles in S. The positions of these peaks are determined by $k_+ L \cos \theta = n\pi$ and $k_- L \cos \theta = n\pi$, and the minimum between the two adjacent peaks is determined by $(k_+ - k_-)L \cos \theta = (2n - 1)\pi$ with n a positive integer, as has been discussed in [15]. These bound states are the results of quantum interferences in the S well between electron-like quasiparticles and those between holelike ones, respectively. The transport coefficients depend to a great extent on the orientation of the crystal of the d-wave S. The main difference between $\alpha = \theta = 0$ and $\alpha = \theta = \pi/4$ is that for the latter there is a zero-bias peak (ZBP) in the AR coefficient since the effective pair potentials felt by the electron-like excitation and holelike excitation have opposite signs. The ZBP splits across gradually with increasing z_0 . For $\alpha = 0$, there is no ZBP in the AR coefficient, and all the coefficients as a function of E are very similar to those in the s-wave case [15].

Figure 3 shows numerical results for transport coefficients as a function of thickness L of the middle S (the left-hand column for $\alpha = \theta = 0$ and the right-hand one for $\alpha = \theta = \pi/4$) with different z_0 at $E = 0$. It is found that for very small L , R_{ee} plus $T_{\text{e'e}}$ is almost equal to unity and $R_{\text{he}} = T_{\text{h'e}} = 0$. In this case, the quasiparticle can directly tunnel through the S interlayer without creation or annihilation of Cooper pairs. Except in the case of $z_0 = 0$, all the coefficients exhibit oscillatory behaviour with L , the oscillation amplitude increasing

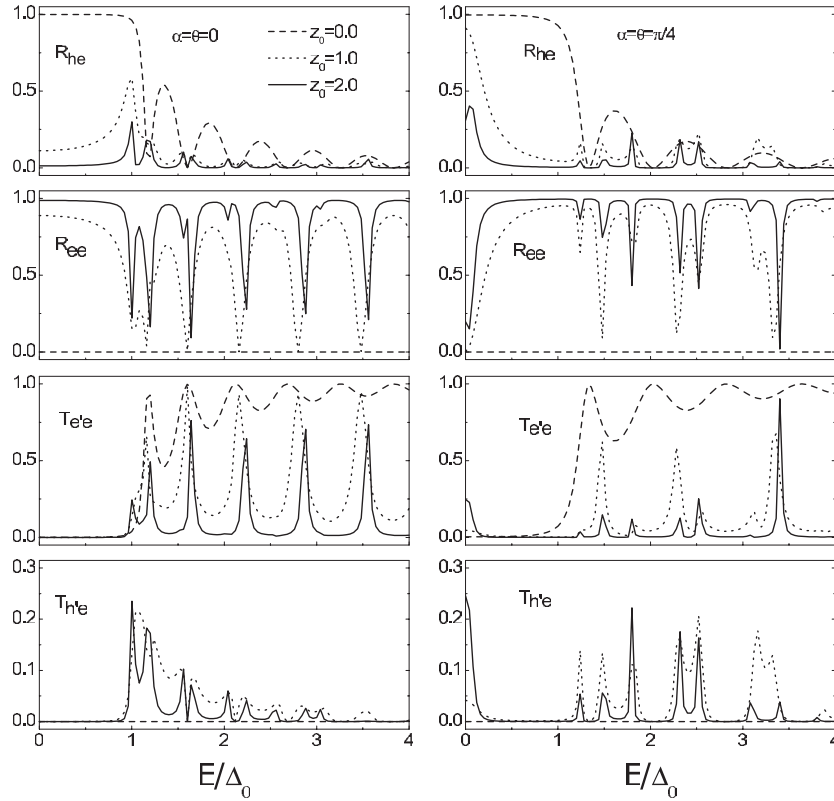


Figure 2. Reflection and transmission probabilities for R_{he} , R_{ee} , $T_{e'e}$, and $T_{h'e}$ as a function of E/Δ_0 at zero temperature for $\theta = \alpha = 0$ in the left-hand column and $\theta = \alpha = \pi/4$ in the right-hand column. Here $E_F/\Delta_0 = 10$ and $k_F L = 100$.

with increasing z_0 . With L increased, the oscillation vanishes gradually, indicating that the quantum interference effects in S may be neglected if L is large enough. For larger z_0 and L , the normal reflection coefficient R_{ee} is close to unity, the AR coefficient R_{he} is small, and the others are zero for $\alpha = 0$; while R_{he} is approaching unity and R_{ee} is almost vanishing for $\alpha = \pi/4$. Such a difference also comes from the crystal-orientation effect of the d-wave S.

3. Tunnelling conductance

Once all the transmission and reflection probabilities are obtained, we can calculate currents in response to a difference in the chemical potential between the two Ns. Assume μ_L and μ_R to be the chemical potentials of the left- and right-hand N electrodes, respectively, and μ the chemical potential of S. Under the bias voltage V ($eV = \mu_L - \mu_R$) applied to the N/S/N structure, and taking into account the four processes shown in figure 1, we get the current from the left-hand N into S as

$$I_L = \frac{2e}{h} \int_0^\infty dE \int_0^{\pi/2} d\theta [f_0(E - e\phi_1)(1 - R_{ee} + R_{he}) + f_0(E - e\phi_2)(T_{hh'} - T_{eh'}) + f_0(E + e\phi_1)(-1 - R_{eh} + R_{hh}) + f_0(E + e\phi_2)(T_{he'} - T_{ee'})] \cos \theta, \quad (6)$$

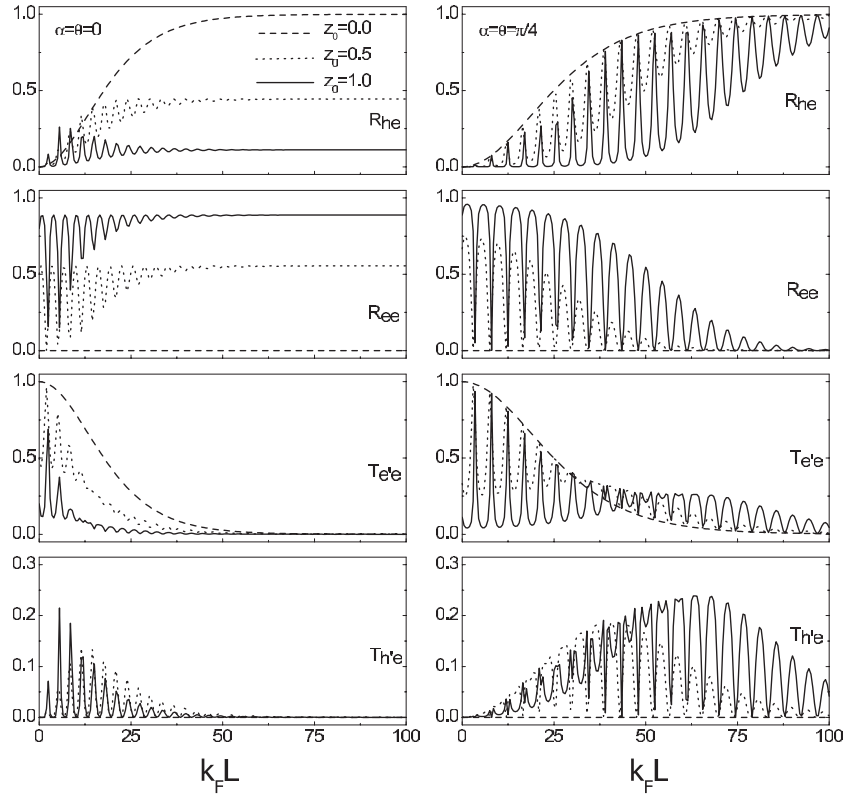


Figure 3. Reflection and transmission probabilities for R_{he} , R_{ee} , $T_{e'e}$, and $T_{h'e}$ as a function of $k_F L$ at zero temperature for $\theta = \alpha = 0$ in the left-hand column and $\theta = \alpha = \pi/4$ in the right-hand column. Here $E_F/\Delta_0 = 10$ and $E = 0$.

where $f_0(E)$ is the Fermi distribution function, $e\phi_1 = \mu_L - \mu$, and $e\phi_2 = \mu - \mu_R$. Similarly, the current from S to the right-hand N is given by

$$I_R = \frac{2e}{h} \int_0^\infty dE \int_0^{\pi/2} d\theta [f_0(E - e\phi_1)(T_{e'e} - T_{h'e}) + f_0(E - e\phi_2)(1 - R_{h'h'} + R_{e'h'}) + f_0(E + e\phi_1)(T_{e'h} - T_{h'h}) + f_0(E + e\phi_2)(-1 - R_{h'e'} + R_{e'e'})] \cos\theta. \quad (7)$$

The current continuous condition requires $I_L = I_R$, from which μ is obtained as $\mu = (\mu_L + \mu_R)/2$. Using the probability conservation conditions $R_{ee} + R_{he} + T_{e'e} + T_{h'e} = 1$, $R_{eh} + R_{hh} + T_{e'h} + T_{h'h} = 1$, $R_{e'e'} + R_{h'h'} + T_{e'e'} + T_{h'e'} = 1$, and $R_{e'h'} + R_{h'h'} + T_{eh'} + T_{hh'} = 1$, we obtain

$$I = \frac{2e}{h} \int_0^\infty dE \int_0^{\pi/2} d\theta \cos\theta (R_{he} + R_{eh} + T_{e'e} + T_{h'h}) \left[f_0\left(E - \frac{eV}{2}\right) - f_0\left(E + \frac{eV}{2}\right) \right]. \quad (8)$$

The differential conductance is given by

$$G = \frac{G_0}{8k_B T} \int_0^\infty dE \int_0^{\pi/2} d\theta \cos\theta (R_{he} + R_{eh} + T_{e'e} + T_{h'h}) W, \quad (9)$$

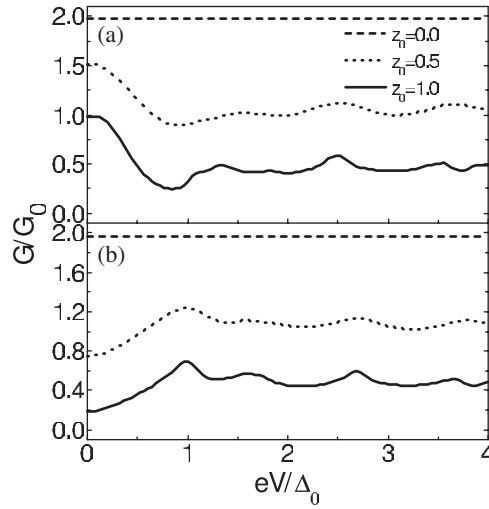


Figure 4. Differential conductance as a function of the bias voltage at zero temperature for $\alpha = \pi/4$ (a) and $\alpha = 0$ (b). Here $E_F/\Delta_0 = 10$ and $k_F L = 50$.

with $G_0 = 2e^2/h$ and

$$W = \cosh^{-2} \left(\frac{2E - eV}{4k_B T} \right) + \cosh^{-2} \left(\frac{2E + eV}{4k_B T} \right). \quad (10)$$

At zero temperature, the differential conductance is reduced to

$$G = G_0 \int_0^{\pi/2} d\theta \cos \theta (R_{he} + R_{eh} + T_{e'e} + T_{h'h})_{E=eV}. \quad (11)$$

Figure 4 shows the differential conductance G as a function of bias voltage eV/Δ_0 for different z_0 at zero temperature, in which $\alpha = \pi/4$ (a) and $\alpha = 0$ (b). For $z_0 = 0$, the value of G/G_0 is constant and equal to two. This result stems from the fact that the coefficients in equation (11) satisfy $R_{he} + T_{e'e} = 1$ and $R_{eh} + T_{h'h} = 1$, as shown in figure 2. As z_0 is increased, the magnitude of G decreases, but the oscillation amplitude increases due to the enhancement of quantum interference effects in S. At finite z_0 , a main difference between $\alpha = \pi/4$ and 0 is that the ZBCP appears for $\alpha = \pi/4$, but does not for $\alpha = 0$. For $eV > \Delta_0$, the differential conductances in both cases are similar to each other.

In order to further clarify features of ZBCP in the N/d-wave S/N junctions, we plot in figure 5 the zero-bias conductance as a function of L for different z_0 with $\alpha = \pi/4$ (a) and $\alpha = 0$ (b). Several interesting features can be found. First, $G(V = 0)$ exhibits damped oscillatory behaviour with increasing L , the oscillation period equal to π/k_F . The oscillating behaviour arises from the quantum interference effects of quasiparticles in S at the Fermi level. Second, with increasing barrier strength z_0 , the magnitude of $G(V = 0)$ is gradually lowered due to the suppression of the AR. Third, in the $\alpha = \pi/4$ case, the magnitude of G/G_0 shows a rising tendency with L , approaching two. This behaviour is similar to that in the N/d-wave S junction. In the case of $\alpha = 0$, however, the magnitude of G/G_0 shows a lowering tendency with L , and it will become zero if both z_0 and L are sufficiently large. This difference again indicates that the appearance of the ZBCP depends on the orientation of the crystal of the d-wave S. In figure 6, we plot the zero-bias conductance as a function of L with different temperatures T/T_c . It is found that the zero-bias conductance is always decreased with increasing temperature.

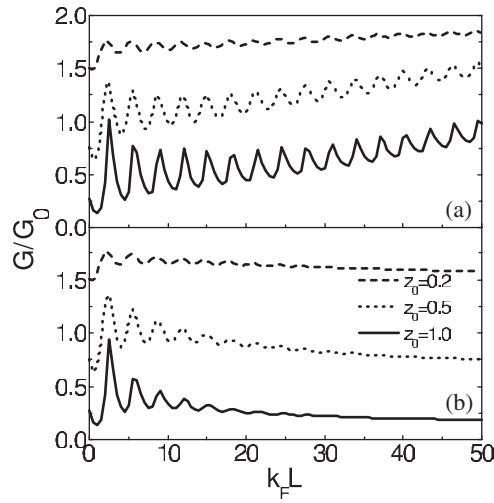


Figure 5. Zero-bias conductance as a function of $k_F L$ at zero temperature for $\alpha = \pi/4$ (a) and $\alpha = 0$ (b) with $E_F/\Delta_0 = 10$.

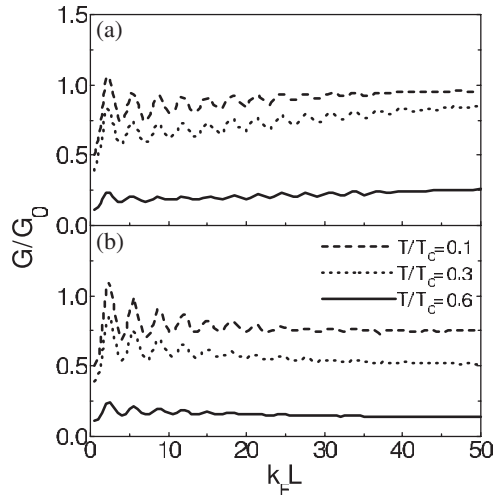


Figure 6. Zero-bias conductance as a function of $k_F L$ at different T/T_c for $\alpha = \pi/4$ (a) and $\alpha = 0$ (b). Here $E_F/\Delta_0 = 10$ and $z_0 = 0.5$.

4. Conclusion

We have studied the coherent tunnelling transport in the N/d-wave S/N double tunnel junctions. The expression for the tunnelling current through the junction is derived by simultaneously taking into account the electron-injected current from one N electrode and the hole-injected current from the other. The quantum interference effects of quasiparticles in the S interlayer give rise to oscillations of the reflection and transmission probabilities as well as the tunnelling conductance with energy. The tunnelling conductance depends strongly on the orientation of the crystal of the d-wave S. For $\alpha = \pi/4$, there appears a ZBCP, an important signature of the

d-wave S. The magnitude of the zero-bias conductance is gradually lowered with increasing barrier strength and/or temperature, exhibiting damped oscillatory behaviour with thickness of S. Since the coherent length of the d-wave S is much shorter than that of the s-wave S, for small thickness of S (e.g., $k_F L = 100$), quasiparticle transport coefficients and differential conductance exhibit characteristic oscillations in N/d-wave S/N double tunnel junctions. In N/s-wave S/N structures, however, only when the thickness of S is taken as very large (e.g., $k_F L = 10\,000$) will there be characteristic oscillations in quasiparticle transport coefficients and differential conductance [15]. Also, there is a ZBCP formed in the N/d-wave S/N tunnel junctions, while no ZBCP appears in the N/s-wave S/N structure. These features may be used to distinguish between d-wave and s-wave Ss. The N/d-wave S/N structures can be made with the development of nanofabrication technique and the improvement of experimental methods. It is expected that the theoretical results obtained will be confirmed in a future experiment. Oscillations of the differential conductance with the period of geometrical resonance could be used for spectroscopy of quasiparticle excitations in S. The present work is an extension of the Blonder–Tinkham–Klapwijk (BTK) approach [26] to the N/S/N double junction. In this double junction, if the thickness of S is longer than the coherent length, there will be a sequent tunnelling, in which the BTK approaches are readily applied to the two independent junctions. In the present coherent tunnelling, the extension of the BTK is never trivial [15, 16]; the quasiparticle interference and resonant tunnelling play an important role. In the present model, we have neglected the spatial variation of the pair potential in S due to proximity effects, scattering effects of interface roughness, and nonequilibrium effects. Inclusion of these effects would be necessary for a complete theory, which merits further study.

Acknowledgments

This work is supported by the National Natural Science Foundation of China under grant numbers 10374046, 10347129, and 10174011. ZCD also thanks the ‘333’ project of Jiangsu Province of China.

References

- [1] Tomasch W J 1965 *Phys. Rev. Lett.* **15** 672
Tomasch W J 1966 *Phys. Rev. Lett.* **16** 16
- [2] Kashiwaya S and Tanaka Y 2000 *Rep. Prog. Phys.* **63** 1641
- [3] Nevirkovets I P, Shafranjuk S E and Ketterson J B 2003 *Phys. Rev. B* **68** 24514
- [4] Andreev A F 1964 *Zh. Eksp. Teor. Fiz.* **46** 1823
Andreev A F 1964 *Sov. Phys.—JETP* **19** 1228 (Engl. Transl.)
- [5] Klapwijk T M, Blonder G E and Tinkham M 1982 *Physica B* **109/110** 1657
- [6] Hoss T, Strunk C, Nussbaumer T, Huber R, Staufer U and Schonenberger C 2000 *Phys. Rev. B* **62** 4079
- [7] Ingerman A, Johansson G, Shumeiko V S and Wendin G 2001 *Phys. Rev. B* **64** 144504
- [8] McMillan W L and Anderson P W 1966 *Phys. Rev. Lett.* **16** 85
- [9] Rowell J M and McMillan W L 1966 *Phys. Rev. Lett.* **16** 453
- [10] McMillan W L 1968 *Phys. Rev.* **175** 559
- [11] Lambert C J 1991 *J. Phys.: Condens. Matter* **3** 6579
- [12] Dong Z C, Xing D Y and Dong J M 2002 *Phys. Rev. B* **65** 214512
- [13] Neshor O and Koren G 1999 *Phys. Rev. B* **60** 9287
- [14] Bozovic M and Radovic Z 2002 *Phys. Rev. B* **66** 134524
- [15] Dong Z C, Shen R, Zheng Z M, Xing D Y and Wang Z D 2003 *Phys. Rev. B* **67** 134515
- [16] Yamashita T, Imamura H, Takahashi S and Maekawa S 2003 *Phys. Rev. B* **67** 94515
- [17] Kashiwaya S, Tanaka Y, Koyanagi M, Takashima H and Kajimura K 1995 *Phys. Rev. B* **51** 1350
- [18] Kashiwaya S, Tanaka Y, Koyanagi M and Kajimura K 1996 *Phys. Rev. B* **53** 2667
- [19] Tanaka Y and Kashiwaya S 1995 *Phys. Rev. Lett.* **74** 3451

-
- [20] Hu C R 1994 *Phys. Rev. Lett.* **72** 1526
- [21] Geers J M E, Hesselberth M B S, Aarts J and Golubov A A 2001 *Phys. Rev. B* **64** 094506
- [22] Baladis I, Buzdin A, Ryzhanova N and Vedyayev A 2001 *Phys. Rev. B* **63** 054518
- [23] Belzig W, Brataas A, Nazarov Y V and Bauer G E W 2000 *Phys. Rev. B* **62** 9726
- [24] de Gennes P G 1966 *Superconductivity of Metals and Alloys* (New York: Benjamin)
- [25] Zhu J X and Ting C S 1999 *Phys. Rev. B* **59** R14165
Zhu J X, Friedman B and Ting C S 1999 *Phys. Rev. B* **59** 9558
- [26] Blonder G E, Tinkham M and Klapwijk T M 1982 *Phys. Rev. B* **25** 4515